Angularly excited and interacting boson stars and Q balls

Yves Brihaye[1,*] and Betti Hartmann[2,†]

[1]*Faculté des Sciences, Université de Mons-Hainaut, 7000 Mons, Belgium*
[2]*School of Engineering and Science, Jacobs University Bremen, 28759 Bremen, Germany*

We study angularly excited as well as interacting nontopological solitons, the so-called Q balls, and their gravitating counterparts, the so-called boson stars, in $3 + 1$ dimensions. Q balls and boson stars carry a nonvanishing Noether charge and arise as solutions of complex scalar field models in a flat space-time background and coupled minimally to gravity, respectively. We present examples of interacting Q balls that arise due to angular excitations, which are closely related to the spherical harmonics. We also construct explicit examples of rotating boson stars that interact with nonrotating boson stars. We observe that rotating boson stars tend to absorb the nonrotating ones for increasing, but reasonably small gravitational coupling. This is a new phenomenon as compared to the flat space-time limit and is related to the negative contribution of the rotation term to the energy density of the solutions. In addition, our results indicate that a system of a rotating and nonrotating boson star can become unstable if the direct interaction term in the potential is large enough. This instability is related to the appearance of ergoregions.

I. INTRODUCTION

Solitons play an important role in many areas of physics. As classical solutions of nonlinear field theories, they are localized structures with finite energy, which are globally regular. In general, one can distinguish topological and nontopological solitons. While topological solitons [1] possess a conserved quantity, the topological charge, which stems (in most cases) from the spontaneous symmetry breaking of the theory, nontopological solitons [2,3] have a conserved Noether charge that results from a symmetry of the Lagrangian. The standard example of nontopological solitons are Q balls [4], which are solutions of theories with self-interacting complex scalar fields. These objects are stationary with an explicitly time-dependent phase. The conserved Noether charge Q is then related to the global phase invariance of the theory and is a function of the frequency. Q can e.g. be interpreted as a particle number [2].

While in standard scalar field theories it was shown that a nonrenormalizable Φ^6 potential is necessary [5], supersymmetric extensions of the standard model (SM) also possess Q-ball solutions [6]. In the latter case, several scalar fields interact via complicated potentials. It was shown that cubic interaction terms that result from Yukawa couplings in the superpotential and supersymmetry breaking terms lead to the existence of Q balls with nonvanishing baryon or lepton number or electric charge. These supersymmetric Q balls have been considered recently as possible candidates for baryonic dark matter [7], and their astrophysical implications have been discussed

[8]. In [9], these objects have been constructed numerically using the exact form of the supersymmetric potential.

Q-ball solutions in $3 + 1$ dimensions have been studied in detail in [5,10,11]. It was realized that, next to non-spinning Q balls, which are spherically symmetric, spinning solutions exist. These are axially symmetric with energy density of toroidal shape and angular momentum $J = kQ$, where Q is the Noether charge of the solution and $k \in \mathbb{Z}$ corresponds to the winding around the z axis. Approximated solutions of the nonlinear partial differential equations were constructed in [5] by means of a truncated series in the spherical harmonics to describe the angular part of the solutions. The full partial differential equation was solved numerically in [10–12] (for a short review see [13]). It was also realized in [5] that in each k sector, parity-even ($P = +1$) and parity-odd ($P = −1$) solutions exist. Parity even and parity odd refer to the fact that the solution is symmetric and antisymmetric, respectively, with respect to a reflection through the x-y plane, i.e. under $\theta \rightarrow \pi - \theta$.

These two types of solutions are closely related to the fact that the angular part of the solutions constructed in [5,10,11] is connected to the spherical harmonic $Y_0^0(\theta, \varphi)$ for the spherically symmetric Q ball, to the spherical harmonic $Y_1^1(\theta, \varphi)$ for the spinning parity-even ($P = +1$) solution, and to the spherical harmonic $Y_2^1(\theta, \varphi)$ for the parity-odd ($P = −1$) solution, respectively. Radially excited solutions of the spherically symmetric, nonspinning solution were also obtained. These solutions are still spherically symmetric but the scalar field develops one or several nodes for $r \in]0, \infty[$. In relation to the apparent connection of the angular part of the known solutions to the spherical harmonics, ''θ-angular excitations'' of the Q balls corresponding to the spherical harmonics $Y_l^k(\theta, \varphi)$,

*yves.brihaye@umh.ac.be
†b.hartmann@jacobs-university.de

$-l \leq k \leq l$ have been constructed explicitly for some values of k and l in [12]. These excited solutions could play a role in the formation of Q balls in the early universe, since it is believed that Q balls forming due to condensate fragmentation at the end of inflation first appear in an excited state and only then settle down to the ground state [14]. The fact that these newly formed Q balls are excited, i.e., in general, not spherically symmetric, could, on the other hand, be a source of gravitational waves [15].

The interaction of two Q balls has also been studied in [12]. It was found that the lower bound on the frequencies ω_i, $i = 1, 2$ is increasing for increasing interaction coupling. Explicit examples of a rotating Q ball interacting with a nonrotating Q ball have been presented.

Complex scalar field models coupled to gravity exhibit a new type of solution, the so-called "boson stars" [16–18]. In [10,11] boson stars have been considered that have flat space-time limits in the form of Q balls.

In this paper, we study interacting boson stars with flat limit solutions in the form of the interacting Q balls that have been studied in [12]. The boson stars are interacting via a potential term, but of course also through gravity.

The paper is organized as follows: in Sec. II we give the model, the Ansatz, and boundary conditions. In Secs. III and IV we discuss our results for Q balls and their gravitating counterparts (boson stars), respectively. Section V contains our conclusions.

II. THE MODEL

In the following, we study a scalar field model coupled minimally to gravity in $3 + 1$ dimensions describing two interacting boson stars. The action S reads

$$S = \int \sqrt{-g} d^4 x \left(\frac{R}{16\pi G} + \mathcal{L}_m \right) \qquad (1)$$

where R is the Ricci scalar, G denotes Newton's constant, and $\mathcal{L}_m$ denotes the matter Lagrangian:

$$\mathcal{L}_m = -\frac{1}{2}\partial_\mu \Phi_1 \partial^\mu \Phi_1^* - \frac{1}{2}\partial_\mu \Phi_2 \partial^\mu \Phi_2^* - V(\Phi_1, \Phi_2), \quad (2)$$

where both Φ_1 and Φ_2 are complex scalar fields and we choose $(- + + +)$ as a signature of the metric. The potential reads

$$V(\Phi_1, \Phi_2) = \sum_{i=1}^{2} (\kappa_i |\Phi_i|^6 - \beta_i |\Phi_i|^4 + \gamma_i |\Phi_i|^2)$$
$$+ \lambda |\Phi_1|^2 |\Phi_2|^2, \qquad (3)$$

where κ_i, β_i, γ_i, $i = 1, 2$ are the standard potential parameters for each boson star, while λ denotes the interaction parameter. The masses of the two bosonic scalar fields are then given by $(m_B^i)^2 = \gamma_i$, $i = 1, 2$.

Along with [10–12], we choose in the following the values

$$\kappa_i = 1, \qquad \beta_i = 2, \qquad \gamma_i = 1.1, \qquad i = 1, 2. \quad (4)$$

In [5] it was argued that a Φ^6 potential is necessary in order to have classical Q-ball solutions. This is still necessary for the model we have defined here, since we want $\Phi_1 = 0$ and $\Phi_2 = 0$ to be a local minimum of the potential. A pure Φ^4 potential which is bounded from below would not fulfill these criteria.

The matter Lagrangian $\mathcal{L}_m$ (2) is invariant under the two independent global U(1) transformations

$$\Phi_1 \rightarrow \Phi_1 e^{i\chi_1}, \qquad \Phi_2 \rightarrow \Phi_2 e^{i\chi_2}. \qquad (5)$$

As such, the total conserved Noether current $j_{(tot)}^\mu$, $\mu = 0, 1, 2, 3$, associated with these symmetries is just the sum of the two individually conserved currents j_1^μ and j_2^μ with

$$j_{(tot)}^\mu = j_1^\mu + j_2^\mu$$
$$= -i(\Phi_1^* \partial^\mu \Phi_1 - \Phi_1 \partial^\mu \Phi_1^*)$$
$$- i(\Phi_2^* \partial^\mu \Phi_2 - \Phi_2 \partial^\mu \Phi_2^*), \qquad (6)$$

with $j_{1\ ;\mu}^\mu = 0$, $j_{2\ ;\mu}^\mu = 0$, and $j_{(tot);\mu}^\mu = 0$.

The total Noether charge $Q_{(tot)}$ of the system is then the sum of the two individual Noether charges Q_1 and Q_2:

$$Q_{(tot)} = Q_1 + Q_2 = -\int j_1^0 d^3 x - \int j_2^0 d^3 x. \qquad (7)$$

Finally, the energy-momentum tensor reads

$$T_{\mu\nu} = \sum_{i=1}^{2} (\partial_\mu \Phi_i \partial_\nu \Phi_i^* + \partial_\nu \Phi_i \partial_\mu \Phi_i^*) - g_{\mu\nu} \mathcal{L}. \qquad (8)$$

A. Ansatz and equations

For the metric, the Ansatz in Lewis-Papapetrou form reads [10]

$$ds^2 = -f dt^2 + \frac{l}{f}\left(g(dr^2 + r^2 d\theta^2) \right.$$
$$\left. + r^2 \sin^2\theta \left(d\varphi + \frac{m}{r} dt \right)^2 \right), \qquad (9)$$

where the metric functions f, l, g, and m are functions of r and θ only. For the scalar fields, the Ansatz reads

$$\Phi_i(t, r, \theta, \varphi) = e^{i\omega_i t + i k_i \varphi} \phi_i(r, \theta), \qquad i = 1, 2, \quad (10)$$

where the ω_i and the k_i are constants. Since we require $\Phi_i(\varphi) = \Phi_i(\varphi + 2\pi)$, $i = 1, 2$, we have $k_i \in \mathbb{Z}$. The mass M and total angular momentum J of the solution can be read off from the asymptotic behavior of the metric functions [10]:

$$M = \frac{1}{2G}\lim_{r \to \infty} r^2 \partial_r f, \qquad J = \frac{1}{2G}\lim_{r \to \infty} r^2 m. \quad (11)$$

The total angular momentum $J = J_1 + J_2$ and the Noether charges Q_1 and Q_2 of the two boson stars are related by $J = k_1 Q_1 + k_2 Q_2$. Boson stars with $k_i = 0$ thus have vanishing angular momentum. Equally, interacting boson stars

with $k_1 = -k_2$ and $Q_1 = Q_2$ have vanishing angular momentum.

The coupled system of partial differential equations is then given by the Einstein equations

$$G_{\mu\nu} = 8\pi G T_{\mu\nu} \qquad (12)$$

with $T_{\mu\nu}$ given by (8) and the Klein-Gordon equations

$$\left(\Box + \frac{\partial V}{\partial |\Phi_i|^2}\right)\Phi_i = 0, \qquad i = 1, 2. \qquad (13)$$

Details about these equations for one complex scalar field can e.g. be found in [10].

B. Boundary conditions

We require the solutions to be regular at the origin. The appropriate boundary conditions read

$$\partial_r f|_{r=0} = 0, \qquad \partial_r l|_{r=0} = 0, \qquad g|_{r=0} = 1,$$
$$m|_{r=0} = 0, \qquad \phi_i|_{r=0} = 0, \qquad i = 1, 2, \qquad (14)$$

for solutions with $k_i \neq 0$, while for $k_i = 0$ solutions, we have

$$\partial_r f|_{r=0} = 0, \qquad \partial_r l|_{r=0} = 0, \qquad g|_{r=0} = 1,$$
$$m|_{r=0} = 0, \qquad \partial_r \phi_i|_{r=0} = 0, \qquad i = 1, 2. \qquad (15)$$

The boundary conditions at infinity result from the requirement of asymptotic flatness and finite energy solutions:

$$f|_{r\to\infty} = 1, \qquad l|_{r\to\infty} = 1, \qquad g|_{r\to\infty} = 1,$$
$$m|_{r\to\infty} = 0, \qquad \phi_i|_{r\to\infty} = 0, \qquad i = 1, 2. \qquad (16)$$

For $\theta = 0$ the regularity of the solutions on the z axis requires

$$\partial_\theta f|_{\theta=0} = 0, \qquad \partial_\theta l|_{\theta=0} = 0, \qquad g|_{\theta=0} = 1,$$
$$\partial_\theta m|_{\theta=0} = 0, \qquad \phi_i|_{\theta=0} = 0, \qquad i = 1, 2, \qquad (17)$$

for $k_i \neq 0$ solutions, while for $k_i = 0$ solutions, we have

$$\partial_\theta f|_{\theta=0} = 0, \qquad \partial_\theta l|_{\theta=0} = 0, \qquad g|_{\theta=0} = 1,$$
$$\partial_\theta m|_{\theta=0} = 0, \qquad \partial_\theta \phi_i|_{\theta=0} = 0, \qquad i = 1, 2. \qquad (18)$$

The conditions at $\theta = \pi/2$ are given by

$$\partial_\theta f|_{\theta=\pi/2} = 0, \qquad \partial_\theta l|_{\theta=\pi/2} = 0, \qquad \partial_\theta g|_{\theta=\pi/2} = 0,$$
$$\partial_\theta m|_{\theta=\pi/2} = 0, \qquad \partial_\theta \phi_i|_{\theta=\pi/2} = 0, \qquad i = 1, 2 \quad (19)$$

for even-parity solutions, while for odd-parity solutions the conditions for the scalar field functions read $\phi_i|_{\theta=\pi/2} = 0$, $i = 1, 2$.

C. Numerical procedure

In the following, we will solve the system of partial differential equations (PDE) (12) and (13) subject to the appropriate boundary conditions given in Sec. II B. This

has been done using the PDE solver FIDISOL [19]. We have mapped the infinite interval of the r coordinate $[0{:}\infty]$ to the finite compact interval $[0{:}1]$ by using the new coordinate $\bar{z} := r/(r + 1)$. We have typically used grid sizes of 150 points in the r direction and 70 points in the θ direction. The solutions presented here have relative errors of 10^{-3} or smaller.

III. Q BALLS

In this section, we study solutions in a flat space-time background; i.e. we choose $G = 0$. The Q balls then interact only via the potential for $\lambda \neq 0$.

A. Single Q balls

In order to be able to understand the structure of a system of two interacting Q balls and their gravitating counterparts, we briefly reconsider the one Q-ball system. This has been studied in great detail in [5,10–12] and arises from our model for $\lambda = 0$ and $\phi_2 \equiv 0$. In this section, we would like to emphasize some of the properties which are important to understand the gravitating case. In the present section on single Q balls, we will omit the index 1, respectively 2, for all quantities. As was noticed in [12]—using spherical coordinates (r, θ, φ) and a standard separation of variables—the solutions to the linearized scalar field equation are given by

$$\phi(r, \theta, \varphi) \propto \frac{J_{l+1/2}(\omega r)}{\sqrt{r}} Y_l^k(\theta, \varphi) \qquad (20)$$

where J denotes the Bessel function and Y_l^k are the standard spherical harmonics with the l integer and $-l \leq k \leq l$. As was shown in [12]—at least for the first few values of k and l—solutions to the full field equations exist in correspondence to the symmetries of the spherical harmonics. Explicit examples of the angular excited solutions have been presented for specific values of k and l. In the following, these solutions will be labeled by the two quantum numbers k and l; i.e. if we use ϕ_l^k, we refer to the solution of the full equation which corresponds to the spherical harmonic Y_l^k.
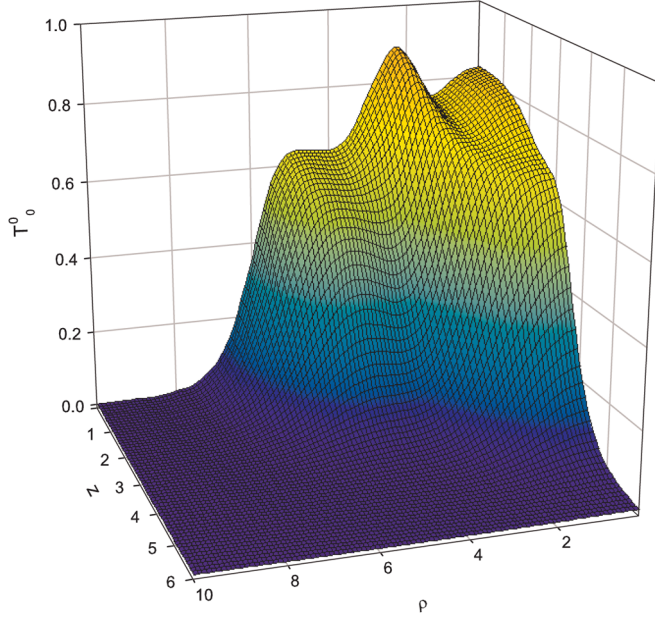
As already stated in Sec. II B, the boundary conditions depend on l, k. Here, we want to state the boundary conditions explicitly together with the parity P of the solution under $\theta \to \pi - \theta$ for the first few values of k and l (see Table I). Let us stress that all these conditions are compatible with the trivial solution $\phi \equiv 0$. Therefore, the numerical construction of nonvanishing solutions turns out to be a nontrivial task. Solutions for the choices of l and k given in Table I have been presented in [12].

B. Interacting Q balls

Interacting Q balls were studied in detail in [12]. The interaction is characterized by the coupling constant λ. The two Q balls decouple in the limit $\lambda = 0$. Here, we want to

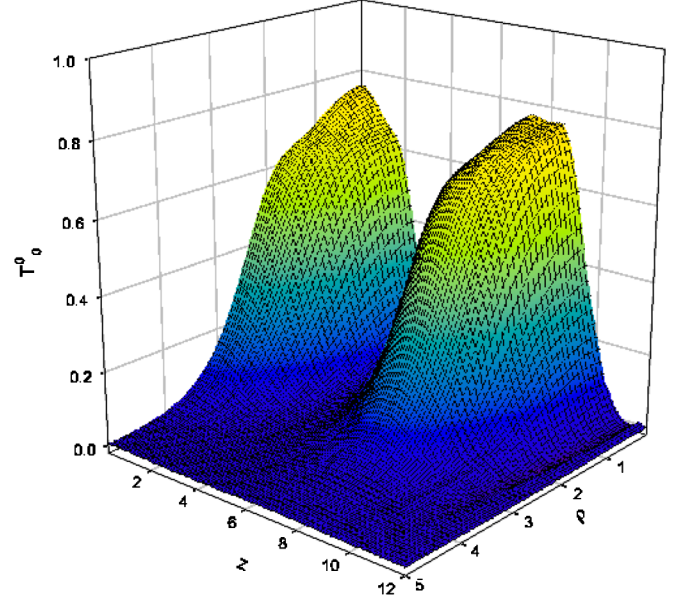TABLE I. Boundary conditions and parity P for different choices of l and k.

l	k	$r = 0$	$r = \infty$	$\theta = 0$	$\theta = \pi/2$	P
0	0	$\partial_r \phi = 0$	$\phi = 0$	$\partial_\theta \phi = 0$	$\partial_\theta \phi = 0$	$-$
1	0	$\partial_r \phi = 0$	$\phi = 0$	$\partial_\theta \phi = 0$	$\phi = 0$	$-$
1	1	$\phi = 0$	$\phi = 0$	$\phi = 0$	$\partial_\theta \phi = 0$	$+$
2	0	$\partial_r \phi = 0$	$\phi = 0$	$\partial_\theta \phi = 0$	$\partial_\theta \phi = 0$	$+$
2	1	$\phi = 0$	$\phi = 0$	$\phi = 0$	$\phi = 0$	$-$

FIG. 1 (color online). The energy density of two interacting Q balls with $l_1 = 0$, $k_1 = 0$ (spherically symmetric, nonrotating) and $l_2 = 1$, $k_2 = 1$ (axially symmetric, rotating, parity even). Here $\lambda = 1$ and $\omega_1 = \omega_2 = 0.8$. Note that we use cylindrical coordinates $z = r\cos\theta$ and $\rho = r\sin\theta$.

present the energy density of some of the solutions in order to illustrate the influence of the interaction term.

In Fig. 1 we present the energy density for a spherically symmetric, nonrotating Q ball interacting with an axially symmetric, rotating and parity-even Q ball for $\lambda = 1$ and $\omega_1 = \omega_2 = 0.8$. Note that we use cylindrical coordinates here with $z = r\cos\theta$ and $\rho = r\sin\theta$. The local maximum appears at $z = 0$, $\rho \approx 2.2$ and is connected to the rotating Q ball. In Fig. 2 we show the energy density corresponding to a spherically symmetric, nonrotating Q ball with $l_1 = 0$, $k_1 = 0$ interacting with an axially symmetric, nonrotating, i.e. angularly excited, Q ball with $l_2 = 1$, $k_2 = 0$. Again, we have chosen $\lambda = 1$ and $\omega_1 = \omega_2 = 0.8$ for this case. The energy density has local maxima at three different values of z. The energy density thus consists of two tori at $z > 0$ and $z < 0$[1] and a deformed spherical ball at $z = 0$.

---

[1]Note that we plot the solution only for $z > 0$, but we can continue it to $z < 0$ due to its symmetry.

FIG. 2 (color online). The energy density of two interacting Q balls with $l_1 = 0$, $k_1 = 0$ (spherically symmetric, nonrotating) and $l_2 = 1$, $k_2 = 0$ (axially symmetric, nonrotating). Here $\lambda = 1$ and $\omega_1 = \omega_2 = 0.8$. Note that we use cylindrical coordinates $z = r\cos\theta$ and $\rho = r\sin\theta$.

IV. BOSON STARS

Once gravity is included ($G \neq 0$), the different possible Q-ball solutions discussed in the previous section become deformed by gravity and are called boson stars. Since only k^2 appears in the equation for the Q ball, the sign of k does not matter and we can restrict ourselves to $k \geq 0$ without losing generality in the flat space-time background case. This changes if we consider solutions in curved space-time, i.e. for $G > 0$. The reason is that the energy-momentum tensor involves terms that are linear in k. Reversing the sign of k, the solutions will have the same energy, but opposite angular momentum.

In the case of interacting boson stars, the situation is more involved: when two boson stars with k_1 and k_2 of the same sign interact, the angular momentum is nonvanishing. However, for $k_1 = -k_2$ the function $m(r, \theta) = 0$ and the total angular momentum is vanishing.

In the presence of gravity, the boson stars interact by means of the direct coupling term in the potential for $\lambda \neq 0$, but also through gravity. To understand the pattern of solutions, we study the energy density in more detail. This reads

$$T_0^0 = V(\phi_1, \phi_2) + \sum_{j=1}^{2} \frac{f}{lg} (\partial_r \phi_j)^2 + \frac{f}{r^2 lg} (\partial_\theta \phi_j)^2$$

$$+ \frac{1}{f} \omega_j^2 \phi_j^2 + \left(\frac{f}{lr^2 \sin^2\theta} - \frac{m^2}{fr^2} \right) k_j^2 \phi_j^2. \quad (21)$$

The important point about this expression is that the term

containing the "rotation function" $m(r, \theta)$ leads to a negative contribution to the energy density. Hence, rotation tends to decrease the energy of the solution.

A. Numerical results

In the following, we will abbreviate $\alpha = 8\pi G$ and focus on the case $\omega_1 = \omega_2$. We have fixed the parameters of the potential according to (4).

1. $l_1 = 0$, $k_1 = 0$, $l_2 = 0$, $k_2 = 0$

This case describes two interacting nonrotating boson stars. The solutions are spherically symmetric. In particular, we find $g(r) = 1$ and $m(r) = 0$. The bound state of two spherically symmetric boson stars with a given value of α behaves roughly as a single boson star with $\alpha/2$. The mass M and the values $\phi_i(0)$ ($i = 1, 2$), $f(0)$, $l(0)$, and $T_0^0(0)$ slowly decrease when the parameter α increases. We found no evidence of a limiting behavior, i.e. no critical α beyond which the solutions cease to exist.

2. $l_1 = 0$, $k_1 = 0$, $l_2 = 1$, $k_2 = 1$

This corresponds to the interaction of a nonrotating boson star and a rotating, axially symmetric and parity-even solution.

The contour plot of a typical solution of this type is presented in Fig. 3 for $\alpha = 0.2$, $\lambda = 0$, and $\omega_1 = \omega_2 = 0.8$. Clearly, the metric functions show nontrivial behavior now.

Varying the gravitational constant α (with all other parameters fixed), our numerical results show that the scalar field function ϕ_1 of the spherically symmetric boson star tends uniformly to zero and that only the spinning boson star survives for sufficiently large α. This result is consistent with the fact that rotation, i.e. nonvanishing $m(r, \theta)$, tends to decrease the energy [see (21)]. The rotating boson star is therefore energetically favored in comparison to the nonrotating case. This phenomenon is, however, strongly related to the gravitational interaction of the two boson stars. Indeed, the nonrotating spherically symmetric boson alone (for $\phi_2 \equiv 0$) exists for (arbitrarily) large values of α. This is illustrated in Fig. 4 for $\lambda = 0$ and $\omega_1 = \omega_2 = 0.8$, where we plot the mass M, charge Q, and $\phi_1(0)$, which corresponds to the maximal value of the scalar field function $\phi_1(r)$ for nonrotating, spherically symmetric solutions The quantities corresponding to interacting boson stars are given by solid lines. $\phi_1(0)$, and with this the field $\phi_1(r)$ corresponding to the nonrotating boson star, becomes identically zero for $\alpha = \alpha_{cr} \approx 0.25$, while the single boson star (dashed lines) exists for much larger values of α. To illustrate this phenomenon further, we also plot the energy density of these solutions for two different values of α in Fig. 5. The solution for $\alpha = 0.1$ shows quite large values for T_0^0 at the origin $\rho = 0$, $z = 0$. Since a nonvanishing contribution to the energy density at the

origin can only come from the spherically symmetric, nonrotating boson star, the contribution of this boson star is still quite strong here. When increasing α, the axially symmetric, rotating boson star tends to absorb the nonrotating one. This is clearly seen when comparing the $\alpha = 0.1$ plot with that for $\alpha = 0.2$. Here, the value of T_0^0 at the origin has decreased strongly and the energy density tends to the shape of a torus, signaling that the spherically symmetric contribution nearly vanishes.

We observe qualitatively the same effect for $\lambda \neq 0$. The critical value of the gravitational coupling α_{cr}, where ϕ_1 becomes identically zero, depends slightly on the coupling constant λ. We find e.g. $\alpha_{cr}(\lambda = 0.5) \approx 0.30$, $\alpha_{cr}(\lambda = 0) \approx 0.25$, and $\alpha_{cr}(\lambda = -0.5) \approx 0.22$, respectively.

Since the appearance of ergoregions for globally regular solutions signals the existence of instabilities [20], we have studied these here as well. The ergoregions of single boson stars have been studied extensively in [11]. Ergoregions exist if the g_{00} component of the metric becomes positive, i.e. for

$$g_{00} = -f + \frac{lm^2}{f}\sin^2\theta \geq 0. \tag{22}$$

We have studied the appearance of ergoregions for $\alpha = 0.1$, $\omega_1 = \omega_2$ and two different values of λ, namely, $\lambda = 0$ and $\lambda = 1.5$, respectively. Our results are shown in Fig. 6. Very similar to the case for fixed $\omega_1 = \omega_2$ and varying α, the spherically symmetric, nonrotating boson star disappears from the solution for $\omega_1 < \omega_{1,cr}$. We demonstrate this by plotting $\phi_1(0)$ [$\phi_1(r)$ has its maximal value at $r = 0$] as a function of ω_1. We find that $\omega_{1,cr}$ decreases with increasing λ, e.g. we find that $\omega_{1,cr} \approx 0.37$ for $\lambda = 0$ and $\omega_{1,cr} \approx 0.35$ for $\lambda = 1.5$. This is easy to understand, since an increasing λ means an increasing direct interaction between the two boson stars. We also plot the maximal value of g_{00}, $g_{00,m}$ as a function of ω_1. Interestingly, for $\lambda = 0$, $g_{00,m}$ stays negative as long as the spherically symmetric boson star is present. Thus for $\alpha = 0.1$ and $\lambda = 0$, there are no instabilities due to ergoregions for those values of $\omega_1 = \omega_2$ where genuine interacting boson stars exist. For smaller values of $\omega_1 = \omega_2$ (and the second branch of solutions), the curve for $g_{00,m}$ would follow the curve for a single rotating boson star given in [11]. The situation changes for $\lambda = 1.5$. Here, $g_{00,m}$ becomes zero at a value of $\omega_1 = \omega_1^{(0)}$ which is larger than the value $\omega_{1,cr}$ at which the spherical boson star disappears from the system. We find $\omega_1^{(0)} \approx 0.38$ for $\kappa = 0.1$ and $\lambda = 1.5$. Thus for $\omega_{1,cr} \leq \omega_1 \leq \omega_1^{(0)}$ the two interacting boson stars possess an ergoregion signaling an instability. It appears that the stronger direct interaction between the boson stars tends to destabilize the system. A more detailed investigation and plots of the ergoregions will be presented in a future publication.
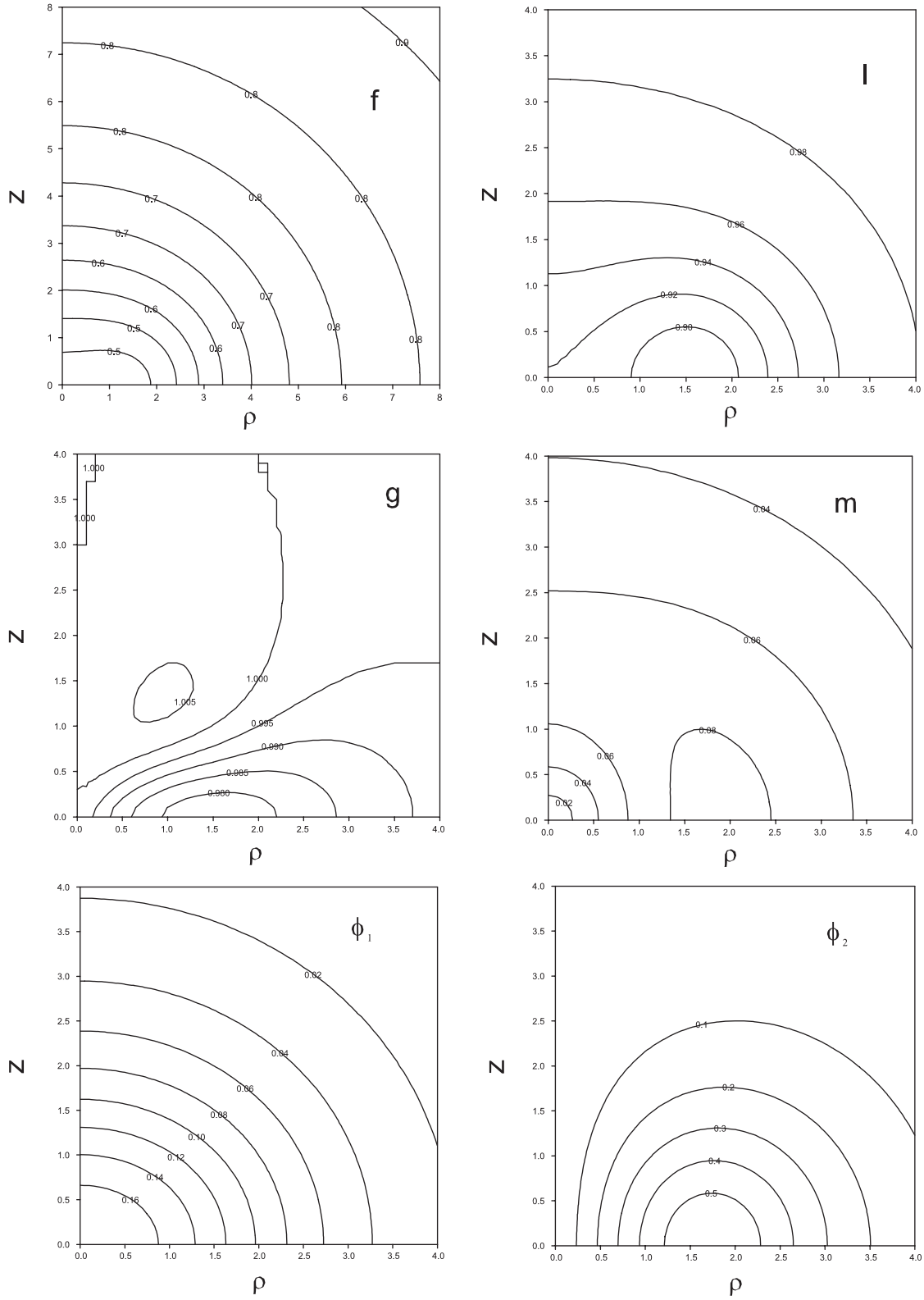
FIG. 3. The contour plots of the metric functions f, l, g, and m as well as of the scalar field functions ϕ_1 and ϕ_2 are shown for two interacting boson stars with $l_1 = 0$, $k_1 = 0$ (spherically symmetric, nonrotating) and $l_2 = 1$, $k_2 = 1$ (axially symmetric, rotating, parity even). Here $\alpha = 0.2$, $\lambda = 0$, and $\omega_1 = \omega_2 = 0.8$. Note that we use cylindrical coordinates $z = r\cos\theta$ and $\rho = r\sin\theta$.
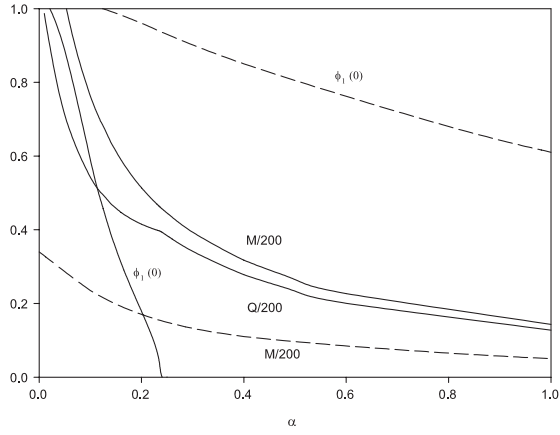
FIG. 4.   The dependence of the mass M, charge Q, and $\phi_1(0)$ on α is shown for two interacting boson stars with $l_1 = 0$, $k_1 = 0$ (spherically symmetric, nonrotating) and $l_2 = 1$, $k_2 = 1$ (axially symmetric, rotating, parity even) (solid lines). Here $\lambda = 0$. For comparison we also give the values for the $l_1 = 0$, $k_1 = 0$ single boson star for which $\phi_2 \equiv 0$ (dashed lines).
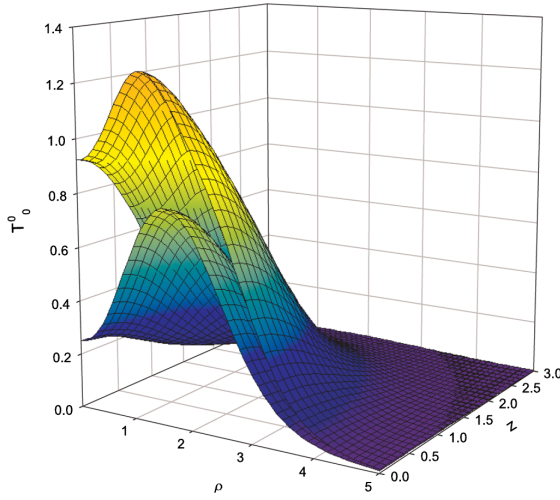

FIG. 5 (color online).   The energy density of two interacting boson stars with $l_1 = 0$, $k_1 = 0$ (spherically symmetric, nonrotating) and $l_2 = 1$, $k_2 = 1$ (axially symmetric, rotating, parity even) for $\alpha = 0.1$ (upper curve) and $\alpha = 0.2$ (lower curve), respectively. Here $\lambda = 0$ and $\omega_1 = \omega_2 = 0.8$. Note that we use cylindrical coordinates $z = r\cos\theta$ and $\rho = r\sin\theta$.
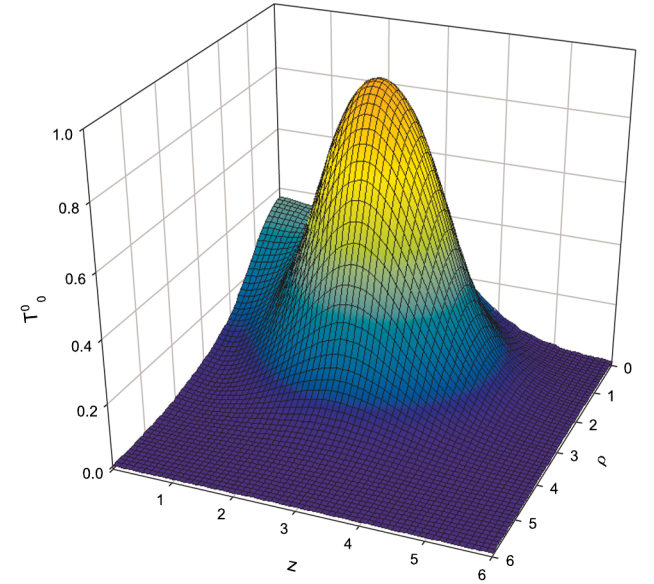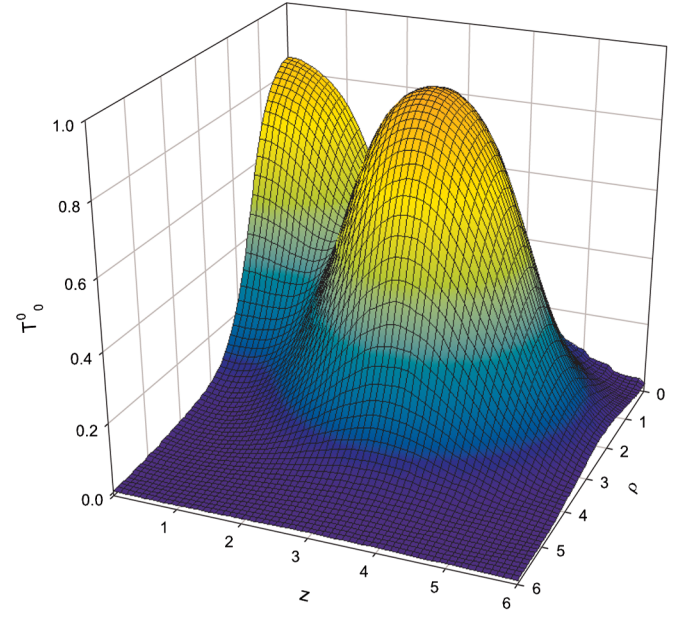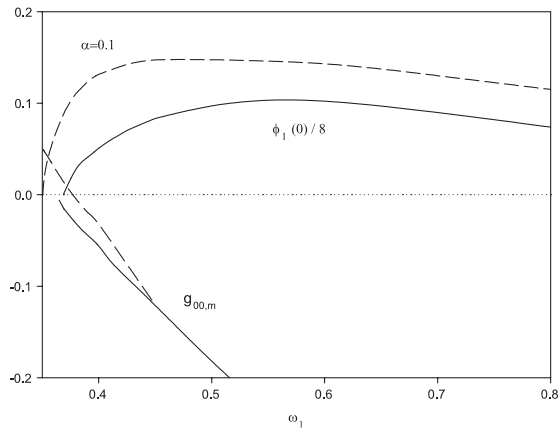

FIG. 7 (color online).   The energy density of two interacting boson stars with $l_1 = 0$, $k_1 = 0$ (spherically symmetric, nonrotating) and $l_2 = 2$, $k_2 = 1$ (axially symmetric, rotating, parity odd). Here $\lambda = 0$, $\omega_1 = \omega_2 = 0.8$, and $\alpha = 0.05$ (top panel), and $\alpha = 0.2$ (bottom panel), respectively. Note that we use cylindrical coordinates $z = r\cos\theta$ and $\rho = r\sin\theta$.

FIG. 6.   The value of the scalar field function at the origin associated with the spherically symmetric boson star $\phi_1(0)$ as well as the maximal value of the time component of the metric $g_{00,m}$ are shown as functions of $\omega_1 = \omega_2$ for $\alpha = 0.1$ and $\lambda = 0$ (solid lines) and $\lambda = 1.5$ (dashed lines), respectively. Here $l_1 = 0$, $k_1 = 0$, $l_2 = 1$, $k_2 = 1$.
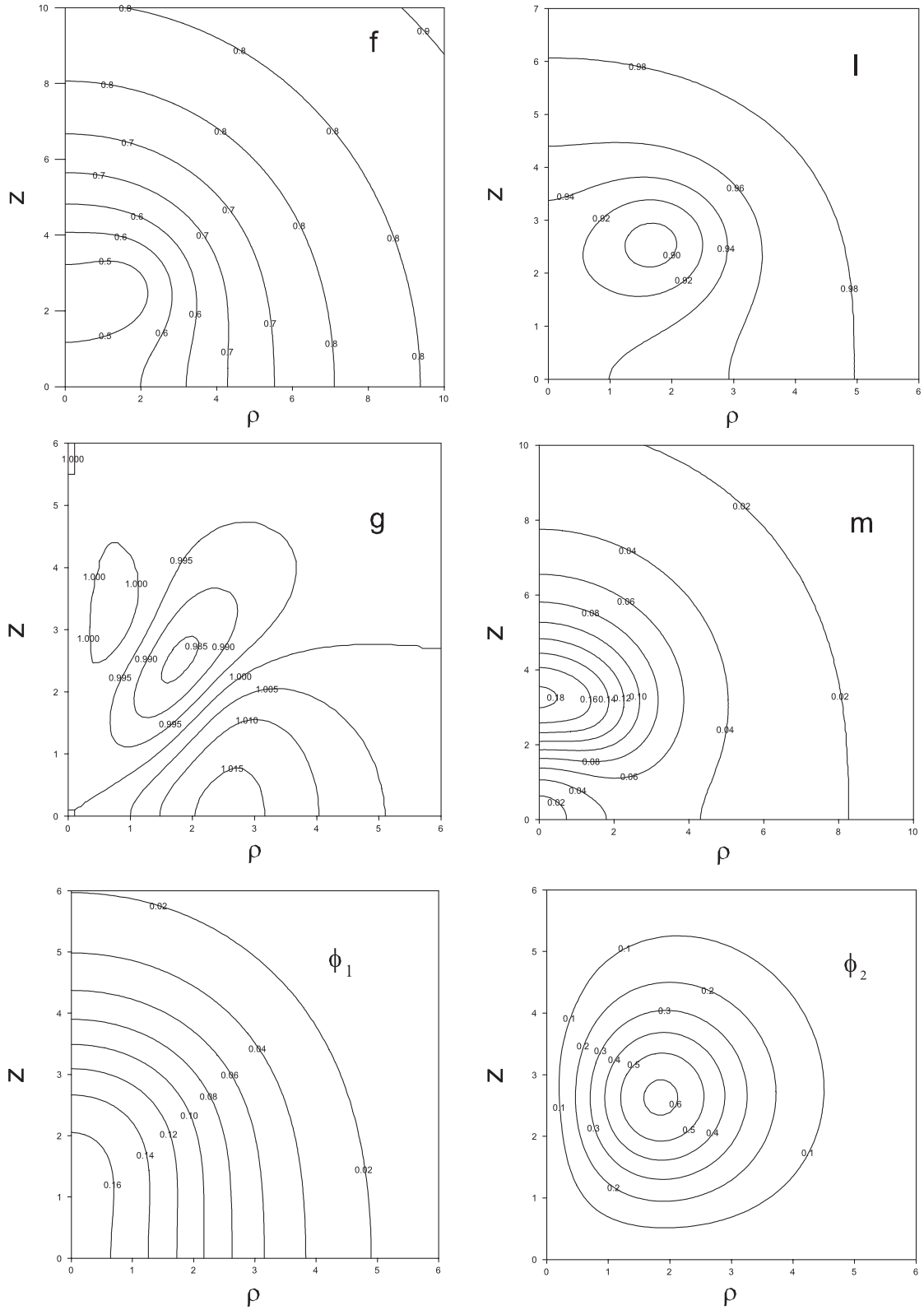
FIG. 8. The contour plots of the metric functions f, l, g, and m, as well as of the scalar field functions ϕ_1 and ϕ_2 are shown for two interacting boson stars with $l_1 = 0$, $k_1 = 0$ (spherically symmetric, nonrotating) and $l_2 = 2$ and $k_2 = 1$ (axially symmetric, rotating, parity odd). Here $\alpha = 0.1$, $\lambda = 0$, and $\omega_1 = \omega_2 = 0.8$.
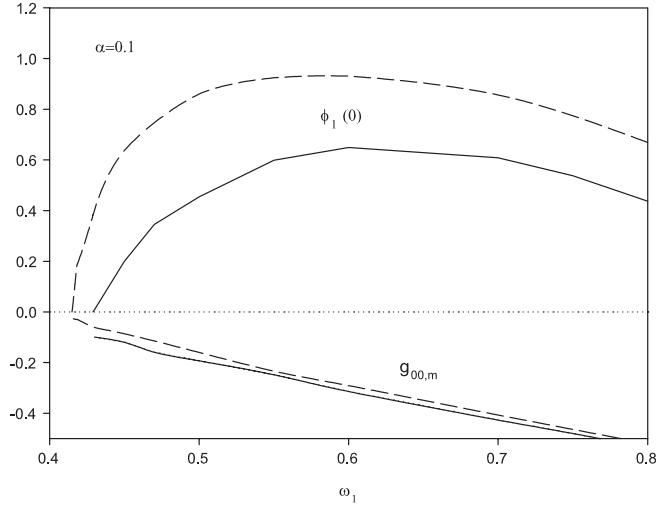
FIG. 9. The value of the scalar field function at the origin associated with the spherically symmetric boson star $\phi_1(0)$ as well as the maximal value of the time component of the metric $g_{00,m}$ are shown as functions of $\omega_1 = \omega_2$ for $\alpha = 0.1$ and $\lambda = 0$ (solid lines) and $\lambda = 1.5$ (dashed lines), respectively. Here $l_1 = 0$, $k_1 = 0$, $l_2 = 2$, $k_2 = 1$.

3. $l_1 = 0$, $k_1 = 0$, $l_2 = 2$, $k_2 = 1$

This corresponds to the interaction of a nonrotating boson star and a rotating, axially symmetric, parity-odd—or in our notation "angularly excited"—solution. The ϕ_2 component corresponding to the rotating boson star is odd under the $z \to -z$ reflection. Our numerical results indicate that this case is qualitatively similar to the previous case. For vanishing and small α the energy density has its maximum in a ball centered around the origin as well as in two tori at $z > 0$ and $z < 0$. This is clearly seen in Fig. 7, where we plot the energy density of the solutions for two different values of α, $\lambda = 0$ and $\omega_1 = \omega_2 = 0.8$. When the parameter α increases, the spherically symmetric boson star disappears and the solution becomes purely axially symmetric. This is indicated in Fig. 7 for $\alpha = 0.2$ and $\alpha = 0.05$. Again for $\alpha = 0.05$, the energy density has a big value at the origin which results from the nonrotating boson star. For $\alpha = 0.2$ this value has decreased significantly and the energy density looks like that of an axially symmetric solution. We also present the contour plots of the metric and matter field functions in Fig. 8 for $\alpha = 0.1$, $\lambda = 0$, and $\omega_1 = \omega_2 = 0.8$.

Considering the ergoregions of these solutions, we find that for $\alpha = 0.1$ and both values of $\lambda = 0$ and $\lambda = 1.5$, respectively, $g_{00,m}$ stays negative for all values of $\omega_1 = \omega_2$ for which genuine interacting boson stars exist. When interacting with a rotating, parity-odd boson star, the spherically symmetric boson star disappears from the solution for values of ω_1 larger than in the case of interaction with a parity-even boson star (see previous section). For $\omega_1 = \omega_2$ smaller than $\omega_{1,\mathrm{cr}}$, i.e. the frequency at which $\phi_1(0)$ [the maximal value of $\phi_1(r)$] vanishes (and for the second branch of solutions), the curve thus follows the curve of the rotating, parity-odd boson star presented in [11]. We find that $\omega_{1,\mathrm{cr}} \approx 0.43$ for $\kappa = 0.1$ and $\lambda = 0$, while $\omega_{1,\mathrm{cr}} \approx 0.41$ for $\kappa = 0.1$ and $\lambda = 1.5$. The corresponding data are plotted on Fig. 9.

V. CONCLUSION

In this paper we have studied angularly excited as well as interacting Q balls and their gravitating counterparts, boson stars. When a nonrotating boson star interacts with a rotating boson star for fixed angular frequency ω and varying gravitational coupling, the nonrotating boson star tends to disappear from the system if the gravitational coupling reaches a critical value. For gravitational couplings above these critical values, only single, axially symmetric boson stars exist. The same holds true if the gravitational coupling is fixed and the angular frequency lowered. Then below a critical value of the angular frequency ω, the nonrotating boson stars have disappeared from the bound system. As a consequence, the bound state of two boson stars with $l_1 = k_1 = 0$ and $l_2 = k_2 = 1$ exists only on a finite domain of the parameter space ω_1, ω_2. We observe that this behavior is qualitatively independent of the choice of the direct interaction parameter λ in the potential.

When considering the existence of ergoregions for our solutions, which would signal an instability, we observe that the two cases of a nonrotating boson star interacting with a rotating, parity-even boson star on the one hand and with a rotating, parity-odd boson star on the other hand are qualitatively different. While in the latter case no ergoregions appear for genuinely interacting boson stars, i.e. with the nonrotating boson star present in the system, ergoregions appear in the former case if the interaction parameter λ is made large enough.

[1] N. S. Manton and P. M. Sutcliffe, *Topological Solitons* (Cambridge University Press, Cambridge, England, 2004).

[2] R. Friedberg, T. D. Lee, and A. Sirlin, Phys. Rev. D **13**, 2739 (1976).

[3] T. D. Lee and Y. Pang, Phys. Rep. **221**, 251 (1992).

[4] S. R. Coleman, Nucl. Phys. **B262**, 263 (1985).

[5] M. S. Volkov and E. Wöhnert, Phys. Rev. D **66**, 085003 (2002).

[6] A. Kusenko, Phys. Lett. B **404**, 285 (1997); **405**, 108 (1997).

[7] See e.g. A. Kusenko, arXiv:hep-ph/0009089.

[8] K. Enqvist and J. McDonald, Phys. Lett. B **425**, 309 (1998); S. Kasuya and M. Kawasaki, Phys. Rev. D **61**, 041301 (2000); A. Kusenko and P. J. Steinhardt, Phys. Rev. Lett. **87**, 141301 (2001); T. Multamaki and I. Vilja, Phys. Lett. B **535**, 170 (2002); M. Fujii and K. Hamaguchi, Phys. Lett. B **525**, 143 (2002); M. Postma, Phys. Rev. D **65**, 085035 (2002); K. Enqvist *et al.*, Phys. Lett. B **526**, 9 (2002); M. Kawasaki, F. Takahashi, and M. Yamaguchi, Phys. Rev. D **66**, 043516 (2002); A. Kusenko, L. Loveridge, and M. Shaposhnikov, Phys. Rev. D **72**, 025015 (2005); Y. Takenaga *et al.* (Super-Kamiokande Collaboration), Phys. Lett. B **647**, 18 (2007); S. Kasuya and F. Takahashi, J. Cosmol. Astropart. Phys. 11 (2007) 019.

[9] L. Campanelli and M. Ruggieri, Phys. Rev. D **77**, 043504 (2008).

[10] B. Kleihaus, J. Kunz, and M. List, Phys. Rev. D **72**, 064002 (2005).

[11] B. Kleihaus, J. Kunz, M. List, and I. Schaffer, Phys. Rev. D **77**, 064025 (2008).

[12] Y. Brihaye and B. Hartmann, Nonlinearity **21**, 1937 (2008).

[13] E. Radu, arXiv:gr-qc/0512094.

[14] S. Kasuya and M. Kawasaki, Phys. Rev. D **62**, 023512 (2000); Phys. Rev. Lett. **85**, 2677 (2000); Phys. Rev. D. **64**, 123515 (2001); T. Multamaki and I. Vilja, Nucl. Phys. **B574**, 130 (2000); K. Enqvist, A. Jokinen, T. Multamaki, and I. Vilja, Phys. Rev. D **63**, 083501 (2001).

[15] A. Kusenko and A. Mazumdar, Phys. Rev. Lett. **101**, 211301 (2008).

[16] E. Mielke and F. E. Schunck, *Proceedings of the 8th Marcel Grossmann Meeting, Jerusalem, Israel, 1997* (World Scientific, Singapore, 1999), p. 1607.

[17] R. Friedberg, T. D. Lee, and Y. Pang, Phys. Rev. D **35**, 3658 (1987).

[18] P. Jetzer, Phys. Rep. **220**, 163 (1992).

[19] W. Schönauer and R. Weiß, J. Comput. Appl. Math. **27**, 279 (1989); M. Schauder, R. Weiß, and W. Schönauer, "The CADSOL Program Package," Universität Karlsruhe, Interner Bericht No. 46/92 (1992); W. Schönauer and E. Schnepf, ACM Trans. Math. Softw. **13**, 333 (1987).

[20] V. Cardoso, P. Pani, M. Cadoni, and M. Cavaglia, Phys. Rev. D **77**, 124044 (2008); J. L. Friedman, Commun. Math. Phys. **63**, 243 (1978); N. Comins and B. F. Schutz, Proc. R. Soc. A **364**, 211 (1978); S. Yoshida and Y. Eriguchi, Mon. Not. R. Astron. Soc. **282**, 580 (1996).